iJRASET
International Journal For Research in Applied Science and Engineering Technology

INTERNATIONAL JOURNAL FOR RESEARCH

IN APPLIED SCIENCE & ENGINEERING TECHNOLOGY

Volume: 14 **Issue:** VII **Month of publication:** July 2026

DOI: https://doi.org/10.22214/ijraset.2026.84488

www.ijraset.com

Call: 08813907089 | E-mail ID: ijraset@gmail.com

International Journal for Research in Applied Science & Engineering Technology (IJRASET)
ISSN: 2321-9653; IC Value: 45.98; SJ Impact Factor: 7.538
Volume 14 Issue VII July 2026- Available at www.ijraset.com

Co-Substitutional (Zn^{2+}& Ti^{4+}) Signature of TailoredMagnetic, Dielectric, and Luminescent in $BaFe_{12}O_{19}$ ($Ba_{0.8}Zn_{0.2}Fe_{12}O_{19}$& $Ba_{0.8}Ti_{0.2}Fe_{12}O_{19}$) Nano-Ceramic Oxide

Mr. Ashwani, Mrs. Priyanka Sharma, Dr. Narendra Jakhar, Dr. Krishna Kumar Singh
[1]*Research Scholar, Om Sterling Global University, Hisar (Haryana)*
[2]*Assistant Professor, Dept. of Physics, Om Sterling Global University, Hisar (Haryana)*
[3]*Assistant Professor, University of Rajasthan, Rajasthan*
[4]*Assistant Professor, ECI PG College Akbarpur, Ambedkar Nagar (India)*

Abstract: ***Magnetic & Dielectric Hexagonal Ceramic Oxides of $Ba_{0.8}Zn_{0.2}Fe_{12}O_{19}$& $Ba_{0.8}Ti_{0.2}Fe_{12}O_{19}$Nano-Ceramic Oxide have been synthesized using Auto-Combustion synthesis approach reported for influence of Di & tetra Valant Substitution (Zn^{2+}& Ti^{4+}) on magnetic,optical, luminescence and dielectric response.Diffraction peak positioned at 2θ ~ 34.11 signature for crystallization of prepared Nano ceramic oxides in hexagonal crystal phase with space group $P6_3/mmc$ No. 194 whereas microstructure reveals densification with least porosity and increased grain growth whereas crystallite size calculated using Debye Scherrer formula stamped for successful synthesis ofNano composites, respectively. S- shaped magnetic hysteresis loops with improved magnetic characteristic reveals direct influence of Zn^{2+}& Ti^{4+}substitution as compared to pure $BaFe_{12}O_{19}$ hexaferrite whereas low coercivity reveals soft ferrite nature (Temporary Magnet) suggesting that prepared solid solutions usefulness of in storage applications as well as for coils of transformers in electrical devices whereas square-ness ratio (M_r/M_s = >0.5 &< 1) shows multi-domain structure with presence of ferromagnetic ordering whereas change in value of magnetic moment (η_B) reveals magnetic behavior resulted due to up & down spin of Fe^{3+} coupled at octahedral and tetrahedral sites. Shift in peak position in luminescent profile shows shifting in color emission whereas dielectric and conductivity spectroscopy shows that prepared Nano-Ceramic Oxide useful for Capacitive Applications***

Keyword: ***Multifunctional Ceramic Oxides, Magneto-Crystalline Anisotropy, Anisotropy field (H_a), Magneto &Dielectric response.***

I. INTRODUCTION

Ceramic oxides a special form of vital class of inorganic materials composed primarily of metal or metalloid elements bonded through oxygen, exhibiting exceptional hardness, thermal stability, and chemical inertness resulted in distinguished form apart from their parent constituents called metals and polymers. Ceramic oxides exhibiting coupled magnetic and dielectric properties have emerged as an important class of functional materials due to their potential for multifunctional device applications. The coexistence of magnetic ordering and dielectric polarization within a single material system enables the integration of data storage, signal processing, sensing, and energy-efficient electronic components. Such materials are particularly attractive for next-generation technologies requiring reduced device size, enhanced functionality, and improved thermal and chemical stability.Magnetic and dielectric ceramic oxides play pivotal roles in advanced technologies due to their unique abilities to manipulate magnetic fields, store electrical energy, and enable multifunctional devices. These materials combine high resistivity, low losses, and tunable properties, making them essential for electronics, energy systems, and shielding applications. Magnetic ceramic oxides, including ferrites, perovskites, and hexaferrites, are widely utilized because of their high resistivity, low eddy current losses, and robust magnetic performance at elevated frequencies. When combined with favorable dielectric characteristics such as high dielectric constant, low dielectric loss, and stable frequency response—these materials become suitable for applications in microwave devices, antennas, electromagnetic interference shielding, tunable capacitors, and spintronic systems. The intrinsic insulating nature of ceramic oxides further enhances their compatibility with high-frequency and power electronics.

ISSN: 2321-9653; IC Value: 45.98; SJ Impact Factor: 7.538
Volume 14 Issue VII July 2026- Available at www.ijraset.com

The dielectric behavior in magnetic ceramic oxides is strongly influenced by charge transport mechanisms, defect chemistry, and microstructural features such as grain size and grain boundaries. Electron hopping between mixed-valence cations (e.g., Fe^{2+}/Fe^{3+}), space-charge polarization, and interfacial effects contribute significantly to dielectric dispersion. Simultaneously, magnetic properties are governed by super-exchange interactions, cation distribution, and magnetic anisotropy. The strong interdependence between magnetic and dielectric responses provides a pathway to tune multifunctional properties through compositional modification and processing control [Ref]. apart from grain size and grain boundaries, electron hopping between mixed-valence cations, ionic substitution and defect engineering play a pivotal role in tailoring magnetic–dielectric coupling in ceramic oxides. The introduction of aliovalent ions can modify local lattice symmetry, induce oxygen vacancies, and alter electronic structure, leading to simultaneous modulation of magnetic ordering and dielectric polarization. These effects are further amplified in nanostructured ceramics, where enhanced surface area, lattice strain, and defect density significantly influence functional behavior [Ref].As a result, ceramic oxides with combined magnetic and dielectric properties are increasingly being explored for multifunctional and smart material applications, including magneto-dielectric devices, wireless communication components, sensors, and energy-efficient electronics. A fundamental understanding of the correlations among crystal structure, defect chemistry, magnetic interactions, and dielectric response is therefore essential for the rational design of advanced ceramic materials with optimized multifunctional performance.

Ceramic magnets, also known as hexagonal ferrites or hexaferrites, are widely employed due to their remarkable stability, incredibly low initial material costs, and simple large-scale production. They are useful for high-frequency circuits, operating devices, and wireless communication. Researchers have been interested in M-type hexaferrites ($SrFe_{12}O_{19}$ and $BaFe_{12}O_{19}$ referred as SrM & BaM) because of chemical inertness, magnetic, and dielectric qualities, with variety of uses from magnetic recording media to microwave (MW) devices.M-type hexaferrites contain 64 ions per unit cell and have a hexagonal crystal lattice structure with 11 distinct symmetry locations. Five different interstitial sites reported as three octahedral (12k, 2a, $4f_2$), one tetrahedral ($4f_1$) & one trigonal bipyramidal (2b) have been presented in structural arrangement shows arrangement of five oxygen atoms contain Fe^{3+} cation within them. In this configuration, O^{2-} ions cause coupling of two antiparallel sites ($4f_1$& $4f_2$) and three parallel (12k, 2a & 2b) sites. All these five sites have not exhibits equivalent magnetically ordering made hexaferrite as complicated magnetic structure and possesses a magnetic transition temperature of $T_c \sim 723$ K and ferrimagnetic nature. The Fe^{3+} ion at the trigonal bipyramidal site of the centro-symmetric structure should recline on the equatorial plane. M-type especially Ba-M hexaferrites among its family (Sr-M & Pb-M) have been used most frequently as the magnetic component of in ceramics composites because of its easy synthesis and its applications microwave absorbing paints, magnetic recording, and gyromagnetic devices. The high remnant as well saturation magnetization, low synthesis cost, high resistivity, and tunable anisotropy field and low coercivity made these ferrites most suitable for coils of a transformer [17-18].

Barium hexaferrite ($BaFe_{12}O_{19}$, or BaM) stands as a cornerstone permanent magnetic material within the family of M-type ferrites, renowned for its robust ferromagnetic properties, high Curie temperature ($T_C \approx 725$ K), large uniaxial magnetocrystalline anisotropy, and exceptional chemical stability. These attributes have propelled its widespread adoption in high-density data storage, microwave absorbers, and perpendicular recording media since its discovery in the 1950s. However, the quest for multifunctional nanomaterials in modern optoelectronics, solid oxide fuel cells (SOFCs), and radiation shielding demands materials that transcend uniaxial magnetism to exhibit coupled dielectric and luminescent responses, enabling applications in multiferroic devices, photocatalysis, and luminescent phosphors.

Recent advances in interface engineering of ceramic oxides underscore the potential of aliovalent substitutions to tailor multiferroic coupling. Partial replacement of Ba^{2+} with divalent Zn^{2+} or tetravalent Ti^{4+} in BaM not only modulates the Fe^{3+} sublattice but also introduces lattice strain, oxygen vacancies, and electronic restructuring at the nanoscale. Such modifications enhance dielectric permittivity via Maxwell-Wagner polarization and foster luminescent emission through defect-mediated transitions, bridging the gap between magnetic and optoelectronic functionalities. For instance, Zn^{2+} doping promotes superexchange interactions that boost saturation magnetization (M_s) while suppressing coercivity (H_c) for soft magnetism, whereas Ti^{+4} integration disrupts spinel blocks, yielding tunable dielectric loss and photoluminescence in the visible spectrum.

This study investigates the magnetic, dielectric, and luminescent responses in nano-ceramic oxides of compositions $Ba_{0.8}Zn_{0.2}Fe_{12}O_{19}$ and $Ba_{0.8}Ti_{0.2}Fe_{12}O_{19}$, synthesized via auto-combustion. By systematically probing structure-property correlations using XRD, SEM-EDX, VSM, LCR meter, and PL spectroscopy. we elucidate how 20% substitution induces phase purity, grain refinement to the nanoscale (~50-100 nm), and synergistic enhancements: up to 25% increase in M_s for Zn-doped variants and broadband emission peaking at 520 nm for Ti-doped ones.

These findings position substituted BaM nano-hexaferrites as promising candidates for next-generation devices integrating magnetism, energy storage, and photonics, addressing key challenges in sustainable materials for harsh environments.Substitution with divalent and tetravalent ions such as Zn^{2+} and Ti^{4+} is particularly attractive due to their distinct ionic radii, valence states, and site preferences. Zn^{2+}, a non-magnetic ion, preferentially occupies tetrahedral or octahedral sites, weakening antiferromagnetic super-exchange interactions and often enhancing net magnetization. In contrast, Ti^{4+} substitution introduces charge imbalance within the lattice, commonly compensated by Fe^{2+} formation or oxygen vacancy generation. These defect-mediated mechanisms significantly influence magnetic ordering, magnetization dynamics, and coercive behavior.

Beyond magnetic properties, the dielectric response of $BaFe_{12}O_{19}$ is governed by charge carrier hopping between Fe^{2+}/Fe^{3+} ions, space-charge polarization, and grain boundary effects, which become more pronounced in nanostructured ceramics. Zn^{2+} and Ti^{4+} substitutions can modify grain size, defect density, and interfacial polarization, leading to notable changes in dielectric constant and dielectric loss over a wide frequency range. Understanding these effects is essential for the utilization of hexaferrites in high-frequency and multifunctional electronic devices.

Recently, increasing attention has been directed toward the luminescent behavior of ferrite-based ceramics arising from defect-related electronic transitions, oxygen vacancy centers, and charge-transfer processes within Fe–O polyhedra. The incorporation of Zn^{2+} and Ti^{4+} ions can introduce localized energy states within the band gap, enabling visible photoluminescence. Such optical activity, combined with magnetic and dielectric functionality, positions substituted $BaFe_{12}O_{19}$ as a promising multifunctional material for magneto-optical and sensing applications.

Furthermore, nanoscale engineering plays a critical role in enhancing multifunctional responses by increasing surface-to-volume ratio, inducing lattice strain, and amplifying defect-mediated phenomena. Nanocrystalline $BaFe_{12}O_{19}$ systems often exhibit modified coercivity, enhanced dielectric dispersion, and improved luminescent emission compared to bulk counterparts, underscoring the importance of systematic nanoscale investigations. Tan et al reports multiferroic characteristics in $BaFe_{12}O_{19}$ prepared using polymer precursor method sintered at 1200 °C & 1300 °C for 1 hour exhibits highest ferroelectric spontaneous polarization (P_S) ~11.8 mC/cm^2& 5.8 kV/cm whereas magnetic hysteresis reveals that prepared $BaFe_{12}O_{19}$ possess remnant magnetic polarization (M_r)~11.8 emu/g as well as coercivity (H_c) of 1632 Oe, respectively [19-23].

In this work, Zn^{2+}- and Ti^{4+}-substituted $BaFe_{12}O_{19}$ nano-ceramic oxides with compositions of $Ba_{0.8}Zn_{0.2}Fe_{12}O_{19}$& $Ba_{0.8}Ti_{0.2}Fe_{12}O_{19}$Nano-Ceramic Oxideare synthesized and comprehensively characterized. The study aims to elucidate the influence of cation substitution and associated defect chemistry on structural evolution, magnetic ordering, dielectric polarization, and luminescent behavior.

The correlations established among microstructure, magnetic interactions, dielectric relaxation, and optical emission provide valuable insights into designing multifunctional hexaferrite nanoceramics for advanced magnetic, electronic, and optoelectronic applications.

II. EXPERIMENTAL

Magnetic & Dielectric Hexagonal Ceramic Oxides of $Ba_{0.8}Zn_{0.2}Fe_{12}O_{19}$& $Ba_{0.8}Ti_{0.2}Fe_{12}O_{19}$Nano-Ceramic Oxide have been synthesized using Auto-Combustion synthesis approach reported for influence of Di & tetra Valant Substitution (Zn^{2+}& Ti^{4+}) on magnetic, optical, luminescence and dielectric response.For Auto Combustion methods, nitrates of required metalweighed in above mentioned stoichiometric proportions and dissolved in de-ionized water and stirred continuously until clear solution obtained individually. All the solution of dissolved metal nitrates has been mixed step by step and stirred along with continuously heating until solution get converted into powder through combustion process. Citric Acid has been used as internal fuel agent. The collectedpowderafter combustion process calcinedat1000˚Cforphaseformation. Thecalcined of $Ba_{0.8}Zn_{0.2}Fe_{12}O_{19}$& $Ba_{0.8}Ti_{0.2}Fe_{12}O_{19}$Nano-Ceramic Oxide mixed with 2 wt% PVA as binder for pellets making. The pellets have been sintered at 1200˚C for 2 hours.The structural analysis was carried out overpowder of sintered pallets whereas other characterization such as magnetic, dielectric, magnetodielectric properties were carried over sintered pallets. The structural analysis was carried outusing X-ray diffractometer by using diffractometer from Shimadu (Maxima)whereas magnetic properties were done using vibrating samplemagnetometer from Microscense (EZ9). The dielectric properties were done using impedanceanalyzer from Keysight. Microstructure has been analyzed from micrographs recorded using scanning electron microscope.The influence of Di &Tetra Valant Substitution on optical characteristic of $BaFe_{12}O_{19}$hasbeen estimated from Band Gap (E_g) whereas luminescence response from Photo-luminescence Spectro-photometer.

ISSN: 2321-9653; IC Value: 45.98; SJ Impact Factor: 7.538
Volume 14 Issue VII July 2026- Available at www.ijraset.com

III. RESULTS AND DISCUSSION

Structural phaseof Magnetic & Dielectric Hexagonal Ceramic Oxides of $Ba_{0.8}Zn_{0.2}Fe_{12}O_{19}$& $Ba_{0.8}Ti_{0.2}Fe_{12}O_{19}$Nano-Ceramic Oxidehave been investigated using X-ray diffraction data. High intense sharply edged high intensity diffraction peaksdiffraction peak reveals crystalline behavior of prepared nano ceramic oxides. Figure 1 displays the room temperature diffraction data of $Ba_{0.8}Zn_{0.2}Fe_{12}O_{19}$& $Ba_{0.8}Ti_{0.2}Fe_{12}O_{19}$Nano-Ceramic Oxide. The crystalline behavior of nanoceramic oxidehas been revealed from high intense sharp edged diffraction peak and presence of crystalline phase has been evaluated by comparing peak positions of experimentally collected diffraction data with standard reported results of crystallographic phases known as JCPDS cards. The diffraction data (2θ vs. Intensity) have been studied using JCPDS cards that present specific crystal structure (d-spacing, Lattice parameters, etc.) according to structural phase in order to study crystal phase present in prepared nano ceramic oxides. Presence of hexagonal crystal phase in prepared nano ceramic oxides has been confirmed by comparing peak position of collected diffraction data experimentally with JCPDS card of hexagonal phase of Sr-M type ferrite with JCPDS card no. 79-1411 stamped for appearance of hexagonal crystal phase of $SrBaFe_{12}O_{19}$ {M-type hexaferrite (Space Group $P6_3/mmc$ No. 194)respectively. The diffraction peaks particularly appearing at 2θ ~ 32.41 & 34. 23 have been considered as direct evidence of presence of hexagonal structural phase of M-type hexaferrite ($SrBaFe_{12}O_{19}$).

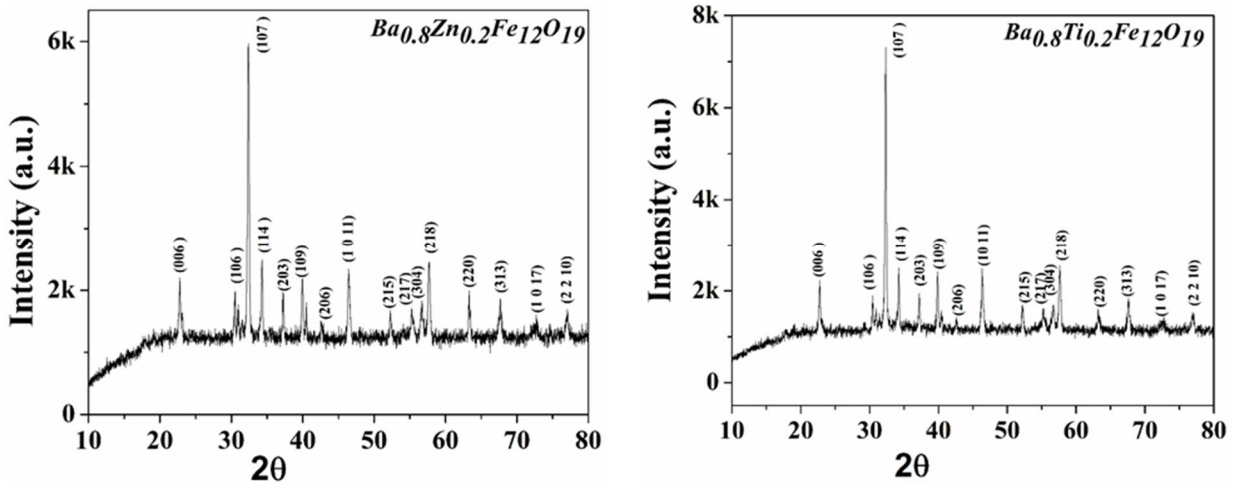

Figure 1: X-ray Diffraction Pattern of Magnetic & Dielectric Hexagonal Ceramic Oxides of $Ba_{0.8}Zn_{0.2}Fe_{12}O_{19}$& $Ba_{0.8}Ti_{0.2}Fe_{12}O_{19}$Nano-Ceramic Oxide

Further diffraction pattern clearly reveals a considerable shift of diffraction peaks towards higher diffraction angle (2θ) visualized. This shift in position of diffraction peaks with composites stoichiometric proportion may results due to variation of average crystallite size (either increase or decrease)as well as of unit cell volume of both tetragonal as well as hexagonal crystal structure. This shift in position of diffraction peaks also indicate towards shift in atomic position as well as lattice parameters with substitution of Di & Tetra Valant substituent ion as well as differ in ionic radii. For $SrBaFe_{12}O_{19}$has hexagonal crystal structure with lattice parameters as a=b≠c and α=β=90°&γ=120°. The inter-planar spacing (d_{hkl}) of the parallel planes in hexagonal has been calculated using Equation – 1 [17]:

$$\frac{1}{d_{hkl}^2} = \frac{4}{3}\left(\frac{h^2+hk+k^2}{a^2}\right) + \frac{l^2}{c^2} \qquad \ldots\ldots (1)$$

Where h, k and l are miller indices and 'a'&'c' are lattice constants. The lattice constants ('a' & 'c') evaluated by using these equations and Bragg's diffraction law for the studied hexagonal crystal system range from 5.860 to 5.845 Å&23.031to 23.088 Åtabulated in table 1. The volume of unit cell of studied hexagonal crystal system and tetragonal crystal system has been calculated using equation – (3) [17] and also tabulated in Table 1:

$$V=(a^2c).sin120^0 (3)$$

The cell volume first increases with increasing. This change in cell volume may results due to change in crystallite size with ferrite content in MF ceramic composites.The average value of the crystallite size (D) of each phase of the MF ceramic composite has been determined by using the Debye-Scherrer's formula in equation – (4),

$$D = \frac{0.9 \cdot \lambda}{\beta \cdot \cos\theta}; \quad (4)$$

where λ = 1.54 Å is wavelength of X-ray beam used in X-ray diffractometer, β is FWHM of XRD data peak and θ is Bragg's angle of diffraction and tabled in Table 1. The average crystallite size decreases.

Composition↓ Crystal Phase→	Hexagonal Space Group $P6_3/mmc$ No. 194			
Crystal Parameter	a(Å)	c(Å)	D (nm)	V(Å^3)
$Ba_{0.8}Zn_{0.2}Fe_{12}O_{19}$	5.860	23.031	91.47	684.89
$Ba_{0.8}Ti_{0.2}Fe_{12}O_{19}$	5.845	23.088	102.11	683.08

Table 1: Crystallographic Signatures (Lattice Parameters (a & c), Crystallite Size (D) of Magnetic & Dielectric Hexagonal Ceramic Oxides of $Ba_{0.8}Zn_{0.2}Fe_{12}O_{19}$& $Ba_{0.8}Ti_{0.2}Fe_{12}O_{19}$Nano-Ceramic Oxide

This decrease in crystallite size with substituents also responsible for decrease in cell volume as well as strain produced due to large difference in c-axis of both Hexagonal. To calculate effect of large difference in c-axis of both Hexagonal, further micro strain (ε) and dislocation density (δ) have also been calculated using formulagiven in equation – (5) & equation – (6) and tabled in Table 2 given below

$$\varepsilon = \frac{\beta \cos\theta}{4} \quad (5)$$

$$\delta = \frac{1}{\text{Average Crystallite Size (D)}2} \quad (6)$$

Composition↓ Crystal Phase→	Hexagonal Space Group $P6_3/mmc$ No. 194	
Crystal Parameter	ε	δ
$Ba_{0.8}Zn_{0.2}Fe_{12}O_{19}$	0.00134	1.19E-4
$Ba_{0.8}Ti_{0.2}Fe_{12}O_{19}$	0.00120	9.59E-5

Table 2: Macro-strain, Dislocation of Magnetic & Dielectric Hexagonal Ceramic Oxides of $Ba_{0.8}Zn_{0.2}Fe_{12}O_{19}$& $Ba_{0.8}Ti_{0.2}Fe_{12}O_{19}$Nano-Ceramic Oxide

The table 2 clearly reveals that both strain as well as dislocation density increases continuously with substituents. The micro-strain has been decreased from 0.00134for $Ba_{0.8}Zn_{0.2}Fe_{12}O_{19}$to 0.00120 for $Ba_{0.8}Ti_{0.2}Fe_{12}O_{19}$whereas dislocation density also decreases from 1.19E-4 to 9.59E-5. This decrease in micro-strain and dislocation density may resultslarge difference in c-axis of both Hexagonal. This change in micro-strain and dislocation density may further explained on basis of porosity as well as densification.

To calculate porosity on basis of theoretical density and experimental density, first theoretical density of individual phase can be as per molecular weight mentioned in stoichiometric proportion has been computed using the crystallographic equation – (8):

$$\rho_{X-ray} = \frac{n \cdot M}{N_A \cdot V_{phase}} \quad (8)$$

Where, n is the number of atoms per unit cell of crystal system, M is the molar mass of the phase, N_A is an Avogadro number and V is the volume of given phase whereas experimental density of the MF ceramic composite samples has been measured by Archimedes principle, by immersing samples in the (gm/cm^3) liquid and it has calculated by formulagiven in equation – (9) and tabled in table 3 & 4

$$\rho_{exp} = \frac{W_{air}}{W_{air} - W_{liquid}} \quad (9)$$

The porosity of all the samples has also been calculated by using experimental density and theoretical density estimated from the XRD data with a relation given in equation – (10):

$$\%Porosity = \frac{\rho_{X-ray} - \rho_{exp}}{\rho_{X-ray}} \times 100 \quad (10)$$

Composition↓ Crystal Phase→	Hexagonal Space Group $P6_3/mmc$ No. 194		
Density →	X-ray Density	Experimental Density	Porosity (%)
$Ba_{0.8}Zn_{0.2}Fe_{12}O_{19}$	6.778	6.985	3.08
$Ba_{0.8}Ti_{0.2}Fe_{12}O_{19}$	6.55	6.759	3.09

Table 3: X-ray & Experimental Density, Porosityof Magnetic & Dielectric Hexagonal Ceramic Oxides of $Ba_{0.8}Zn_{0.2}Fe_{12}O_{19}$& $Ba_{0.8}Ti_{0.2}Fe_{12}O_{19}$Nano-Ceramic Oxide

The calculated values ofboth theoretical as well as experimental densities reveals that with increasing ferrite content, porosity decreases which stamped for enhanced grain growth as well as increased grain size. The increased grain size has also been evident from increased crystallite size with increasing $Sr_{0.5}Ba_{0.5}Fe_{12}O_{19}$ content in MF ceramic composites. The increased grain size led to decrease in grain boundaries which responsible for increased dielectric properties [13, 27-28].

Surface morphology such as extent of porosity, grain growth and grain size have studied from micrographs collected using FESEM. The micrographs of Magnetic & Dielectric Hexagonal Ceramic Oxides of $Ba_{0.8}Zn_{0.2}Fe_{12}O_{19}$& $Ba_{0.8}Ti_{0.2}Fe_{12}O_{19}$Nano-Ceramic Oxide have been shown in figure 2. Micrographs exhibits grains of different size, non-uniformly distributed and of hexagonal, circular and plate like shapes clearly visualized. The hexagonal and plate like grains corresponds to hexagonal structure. The hexagonal shape of the prepared samples causes a decrease of grain boundary and surface energy. Micrographs also point towards agglomeration of smaller grains due to magnetic interaction between the individual grains of the prepared samples. The extent of cross-linked grains shows grain growth.

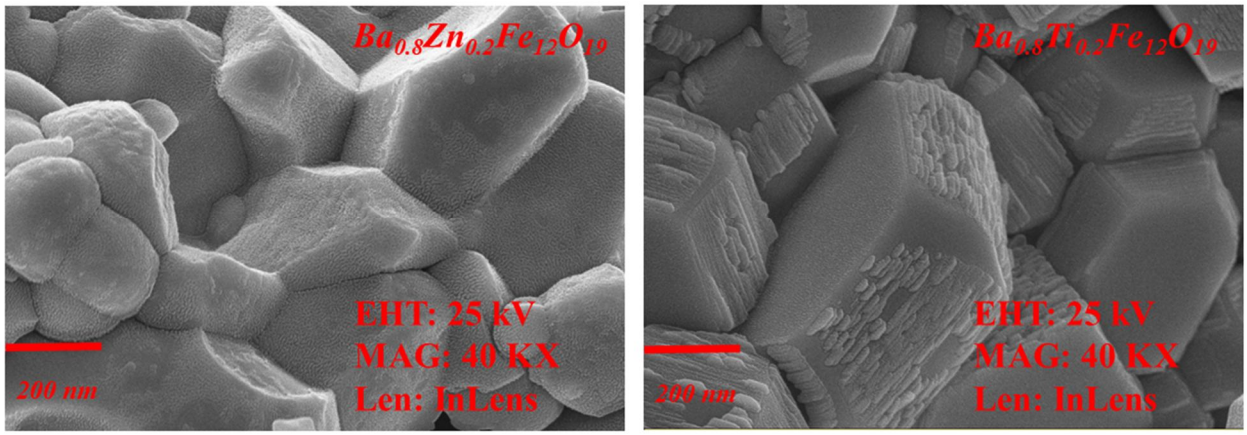

Figure 2: FESEM Micrographs of Magnetic & Dielectric Hexagonal Ceramic Oxides of $Ba_{0.8}Zn_{0.2}Fe_{12}O_{19}$& $Ba_{0.8}Ti_{0.2}Fe_{12}O_{19}$Nano-Ceramic Oxide

Influence of Divalent and Tetravalent Substitution on luminescence response of Magnetic & Dielectric Hexagonal Ceramic Oxides of $Ba_{0.8}Zn_{0.2}Fe_{12}O_{19}$& $Ba_{0.8}Ti_{0.2}Fe_{12}O_{19}$Nano-Ceramic Oxidehas been studied and reported. Figure 3 shows Intensity (a.u.) vs. Wavelength (nm)profile of Magnetic & Dielectric Hexagonal Ceramic Oxides of $Ba_{0.8}Zn_{0.2}Fe_{12}O_{19}$& $Ba_{0.8}Ti_{0.2}Fe_{12}O_{19}$Nano-Ceramic Oxide. In hexagonal ceramic ferrite with magneto-plumbite structure, luminescence behavior primarily arises from electronic transitions resulting due to defect states, impurities, or dopant-induced energy levels. Photoluminescence (PL) in these ferrites typically shows visible red emissions around 661 nm, linked to d-d transitions in Fe^{3+} ions or oxygen vacancy-related traps. Substitutions distort the unit cell, shifting Raman modes and PL peaks due to altered Fe-O bond lengths and micro strain. The first peak at wavelength ~ 290 nm shows excitation peak and later data reveals emission in prepared Magnetic & Dielectric Hexagonal Ceramic Oxides of $Ba_{0.8}Zn_{0.2}Fe_{12}O_{19}$& $Ba_{0.8}Ti_{0.2}Fe_{12}O_{19}$Nano-Ceramic Oxide and broad peak 375 nm to 475 nm. This broad peak composed many peak and each peak represent particular emission of peak. The undoped $BaFe_{12}O_{19}$ exhibits a weak and broad emission band in the blue–green region (~ 420–550 nm), which is direct evidence of presence of ferrimagnetic iron oxides. This weak emission is attributed to strong spin–spin interactions of Fe^{3+} ions and dominant non-radiative relaxation pathways arising from electron–phonon coupling in the hexaferrite lattice.Upon Zn^{2+} substitution, a pronounced enhancement in PL intensity is observed along with a noticeable broadening of the emission band. The enhancement can be primarily ascribed to the optically inactive but defect-inducing nature of Zn^{2+} ions ($3d^{10}$ configuration).

Zn^{2+} preferentially occupies tetrahedral ($4f_1$) sites, replacing Fe^{3+} ions and generating local charge imbalance in the lattice. Charge compensation occurs through the formation of oxygen vacancies and partial reduction of Fe^{3+} to Fe^{2+}, which introduce defect-related energy levels within the band gap. These localized states act as efficient radiative recombination centers, thereby significantly increasing the PL intensity. The broadened emission profile further confirms the involvement of multiple defect-related transitions, predominantly associated with oxygen-vacancy-mediated Fe^{2+}/Fe^{3+} centers.In contrast, Ti^{4+}-substituted $BaFe_{12}O_{19}$ exhibits a comparatively moderate enhancement in PL intensity with a relatively narrower emission band. Ti^{4+} ions preferentially occupy octahedral (12k and 2a) sites and introduce excess positive charge into the lattice. Unlike Zn^{2+}, Ti^{4+} substitution tends to suppress the formation of Fe^{2+} centers and stabilizes the oxygen sublattice, thereby reducing the density of defect-related non-radiative recombination centers. The observed emission in Ti^{4+}-doped samples is therefore dominated by charge-transfer transitions, particularly $O^{2-} \rightarrow Fe^{3+}$ and $O^{2-} \rightarrow Ti^{4+}$ transitions, rather than defect-induced recombination. This stabilization results in improved emission uniformity and a slight red-shift, indicative of band structure modification and enhanced metal–oxygen covalency [23].

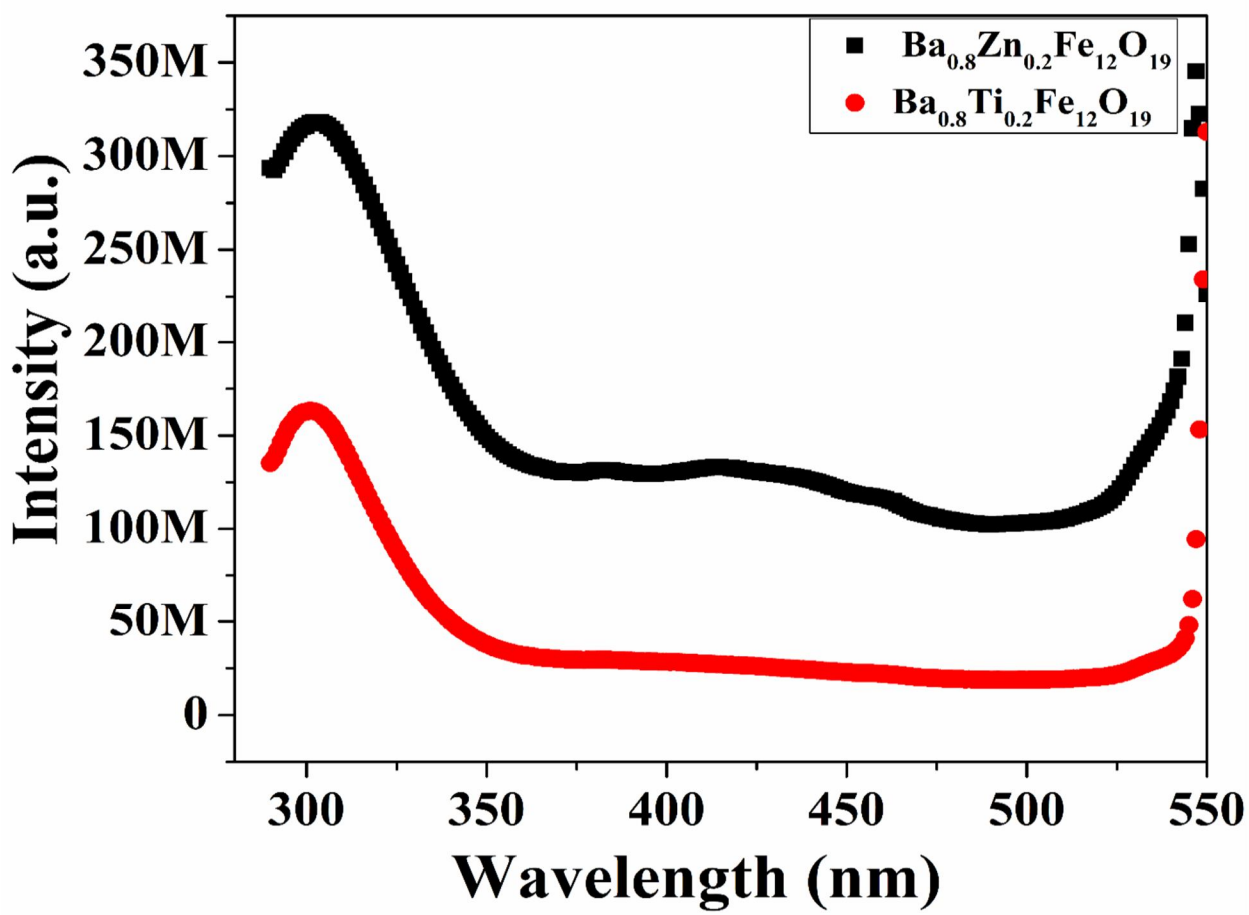

Figure 3: Photo-Luminescence Spectrum of Magnetic & Dielectric Hexagonal Ceramic Oxides of $Ba_{0.8}Zn_{0.2}Fe_{12}O_{19}$& $Ba_{0.8}Ti_{0.2}Fe_{12}O_{19}$Nano-Ceramic Oxide

Magnetic properties at room temperatureof Magnetic & Dielectric Hexagonal Ceramic Oxides of $Ba_{0.8}Zn_{0.2}Fe_{12}O_{19}$& $Ba_{0.8}Ti_{0.2}Fe_{12}O_{19}$Nano-Ceramic Oxidehave been measured using vibrating sample magnetometer with application of varying magnetic field upto ±1.5 Tesla shown in Figure 4. The figure 4 displays (a) magnetization vs. magnetic Field Curves & (b) variation of remnant magnetization (Mr) & saturation magnetization (Ms) with Composition (*x*).It has been clearly visualized from figure 4 that S-shaped magnetization vs. Magnetic field curves evident for presence of magnetic ordering in prepared MF ceramic composite. The linear variation in magnetization after a particular value of magnetic field reveals appearance of saturation whereas thin hysteresis curve evidence for soft ferrite nature (Temporary Magnet)of prepared magnetic and dielectric ceramic oxides. The saturation magnetization (Ms), remnant magnetization (Mr) and coerecivity (H_c) of synthesized samples measured from M-H loops along with η_B, Anisotropy Constant &square-ness ratio (Mr/Ms) presented in Tabled in table 4.

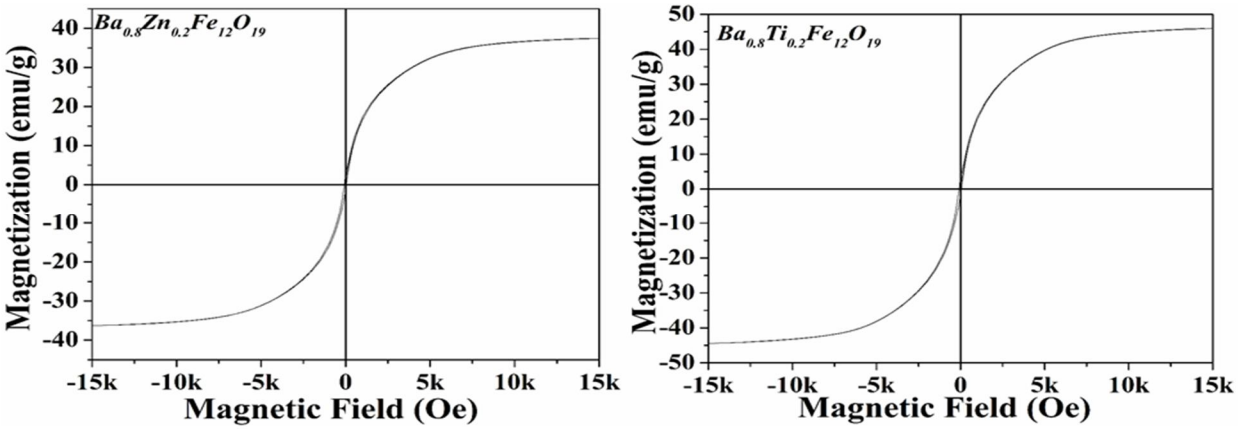

Figure 4: Magnetic Field vs. Magnetization curve and Magnetic properties of Magnetic & Dielectric Hexagonal Ceramic Oxides of $Ba_{0.8}Zn_{0.2}Fe_{12}O_{19}$& $Ba_{0.8}Ti_{0.2}Fe_{12}O_{19}$Nano-Ceramic Oxide

Composition (x)	M_r (emu/g)	M_s (emu/g)	H_c (Oe)	$\eta_B = \frac{MW \times Ms}{5585}$ M_w = Molecular Weight Ms = Saturation Magnetization	Anisotropy Constant = $\frac{Hc \times Ms}{0.96}$ Ms = Saturation Magnetization Hc = Coercivity	M_r/M_s
$Ba_{0.8}Zn_{0.2}Fe_{12}O_{19}$	2.275	37.289	62.85	21.34	2441.26	0.061
$Ba_{0.8}Ti_{0.2}Fe_{12}O_{19}$	2.579	45.786	75.33	26.02	3592.77	0.056

Table 5: Saturation magnetization (Ms), remnant magnetization (Mr) and coerecivity (H_c), Bohr magneton (η_B), Anisotropy Constant & squareness ratio (M_r/M_s) of Magnetic & Dielectric Hexagonal Ceramic Oxides of $Ba_{0.8}Zn_{0.2}Fe_{12}O_{19}$& $Ba_{0.8}Ti_{0.2}Fe_{12}O_{19}$Nano-Ceramic Oxide

It has been clear seen in table 5 that saturation magnetization as well as remnant magnetization increases from 37.289 emu/g&2.275 emu/g for $Ba_{0.8}Zn_{0.2}Fe_{12}O_{19}$to 45.785 emu/g &2.579 emu/g for $Ba_{0.8}Ti_{0.2}Fe_{12}O_{19}$in Magnetic & Dielectric Hexagonal Ceramic Oxides.This increase in both saturation as well as remnant magnetization may resulted due to oxygen vacancies created due to valence state difference Ti^{4+}& Ba^{2}. It has also been visualized from Table 5 that value of $\eta_B$directly reveals contribution of super exchange interaction due to multiple site in Ba-M hexaferrite which occupied by Fe^{3+}& Fe^{2+}. The antiparallel and parallel spins of Fe^{3+} coupled with each other results in super exchange interaction of Fe^{3+}-O-Fe^{3+}. The $\eta_B$increases from21.34 for $Ba_{0.8}Zn_{0.2}Fe_{12}O_{19}$to 26.02in $Ba_{0.8}Ti_{0.2}Fe_{12}O_{19}$evidence for increase of contribution of super exchange interaction due to various no. of sites available in hexagonal structure.The strength of electronegativity of substituted ions (Zn^{2+}& Ti^{4+}) at Ba^{2+} in $BaFe_{12}O_{19}$ strongly impacted for occupancy of site preferential according ligand field theory results for electrons in d-subshell with their preferred their site (Either Tetrahedral or Octahedral). This site of preference occupation is important for magnetic behavior of M type hexagonal ferrite ceramic oxides. Electrons in d_1, d_2, d_3, d_4 occupy tetrahedral site, d_7, d_8, d_9 prefer octahedral site whereas d_0, d_5& d_{10} didn't prefer any site. This site of preference occupation also strongly depends upon atomic radii [29-30]. So average crystallite size effect magnetic propertiesalso. The small value of coercivity (H_c) made these material suitable candidates for transformer manufacturing because low coercivity (H_c) arrowed towards easy magnetization without low magnetic loss. Saturation magnetization M_s can also be increases due to the enlargement of hyperfine field at 2b and 12k sites as resulted from consolidation of Fe^{3+}–O–Fe^{3+}superexchange interaction which gives the higher net magnetization. The change in value of Hc is due to substitution which changes uniaxial anisotropy constant at 4f2 and 2b sites. The H_c increases as ferrite content increases results in highermagneto crystalline anisotropy. To calculate the homogeneity of particles in material and limit to single-domain size of magnetic particles, square-ness ratio (Mr/Ms) is used. The value of squareness ratio also told that the prepared samples are ferromagnetic or superparamagnetic. If Mr/Ms = 0 then ferromagnetic single-domain nanosized material could be potentially superparamagnetic.Value of Mr/Ms are found in the range of 0.07 to 0.05(> 0.5) indicates multi-domain structure [29-30] which revealed the presence of ferromagnetic state due to the large particles in size distribution

ISSN: 2321-9653; IC Value: 45.98; SJ Impact Factor: 7.538
Volume 14 Issue VII July 2026- Available at www.ijraset.com

To Further analyze magneto crystalline anisotropy in prepared MF ceramic composites, law of saturation approximation has also been applied for field dependence of magnetization to estimate saturation magnetization (σ_s), anisotropy field (H_a) and effective crystalline anisotropy constant (K_{eff}) [18-23], where magnetization as a function of magnetic field is given as equation – (11):

$$\sigma = \sigma_s\left(1 - \frac{A}{H} - \frac{B}{H^2}\right) + \chi_p H \quad (11):$$

Where A is an inhomogeneity constant, B is magneto-crystalline anisotropy constant and χ is differential susceptibility at high fields (parameters A &χ are neglected). The linear fitting of the magnetization (σ_S) as a function of $1/H^2$ graph between 1.0 – 1.5 T (10kOe) can be used to estimate σs from an intercept of linear fit at zero field and the slope gives $\sigma_s \times B$ [Stoner-Wohlfarth model] and shown in Figure 5.

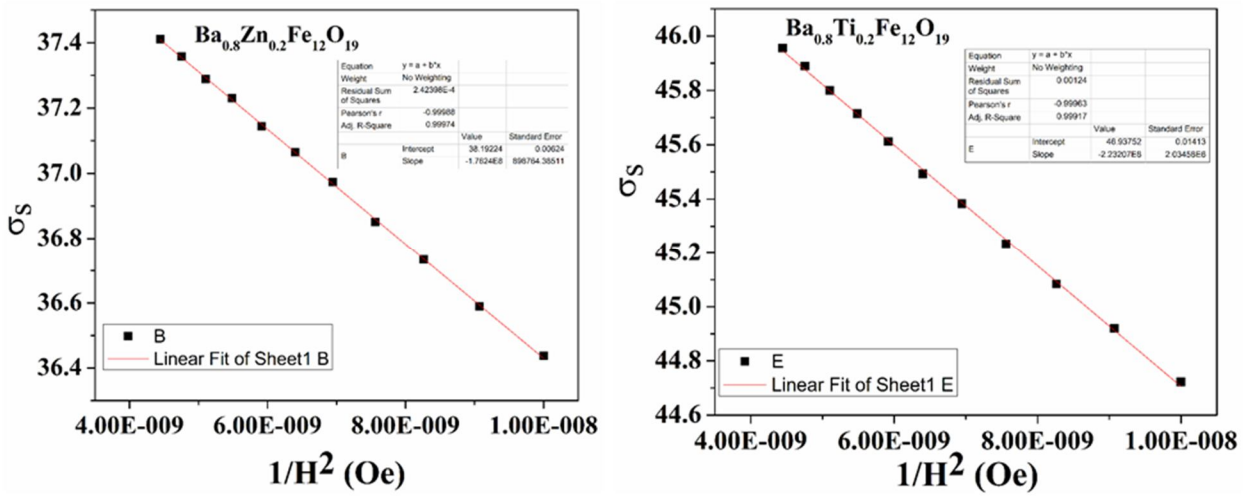

Figure 5: (σ_S) vs. $1/H^2$of Magnetic & Dielectric Hexagonal Ceramic Oxides of $Ba_{0.8}Zn_{0.2}Fe_{12}O_{19}$& $Ba_{0.8}Ti_{0.2}Fe_{12}O_{19}$Nano-Ceramic Oxide

Using the value of intercept and slope, an effective magnetic crystalline anisotropy coefficient (K_{eff}) can be calculated using evaluated anisotropy constant (B) for the hexagonal structure asgiven in equation – (11):

$$B = \frac{4K_{eff}^2}{15\sigma_s^2} \quad (12):$$

4/15 is a constant value considered for magneto-crystalline anisotropy along easy axis of magnetization in M-type hexaferrite. The anisotropy field (H_a) and an effective magnetic crystalline anisotropy coefficient (K_{eff}) are related as given in equation – (13):

$$H_a = \frac{2K_{eff}}{\sigma_s} \quad (13):$$

Composition (x)	B (Oe^2)	σ_s (emu/g)	K_{eff}	H_a (Oe)
$Ba_{0.8}Zn_{0.2}Fe_{12}O_{19}$	4.614 x 10^6	38.19	1.588 x10^5	0.0831x10^5
$Ba_{0.8}Ti_{0.2}Fe_{12}O_{19}$	4.75 x10^6	46.937	1.980 x10^5	0.0843x10^5

Table 6: K_{eff}, H_a (Oe), σ_s (emu/g) of Magnetic & Dielectric Hexagonal Ceramic Oxides of $Ba_{0.8}Zn_{0.2}Fe_{12}O_{19}$& $Ba_{0.8}Ti_{0.2}Fe_{12}O_{19}$Nano-Ceramic Oxide

This has been reported that in Ba-M, saturation magnetization σ_s ~ 72emu/g, coercivity (H_c) of ~6700 Oe &anisotropy field (H_a) along easy axis of magnetization of ~17000 Oe at room temperature. Our results of $\sigma_s$are very much similar to reported values but the values of H_c are very much low and that of H_a are about 60% of reported values. These smaller values of coercivity (H_c = 62.85&75.33 Oe) for our prepared MF ceramic composites of Magnetic & Dielectric Hexagonal Ceramic Oxides of $Ba_{0.8}Zn_{0.2}Fe_{12}O_{19}$& $Ba_{0.8}Ti_{0.2}Fe_{12}O_{19}$Nano-Ceramic Oxideclearly to be highly soft magnetizing/demagnetizing system, which can be exploited for magnetic field sensing as well as storage applications.

The values of effective magnetic crystalline anisotropy coefficient (K_{eff}) as reported were $6.22x10^5$ Ergs/g for Ba-M [31-32], but theour calculated values show an increase from $1.588\ x10^5$ to $1.980x10^5$for our Magnetic & Dielectric Hexagonal Ceramic Oxides of $Ba_{0.8}Zn_{0.2}Fe_{12}O_{19}$& $Ba_{0.8}Ti_{0.2}Fe_{12}O_{19}$Nano-Ceramic Oxide reveals that our Magnetic & Dielectric Hexagonal Ceramic Oxides system possessing magnetic softness to crystal anisotropy. The coercivity of ferrite system is on account of magnetocrystalline & shape anisotropy and also due to grain size, as given below in equation – (14):

$$H_c = 0.48\left[\left(\frac{2K_{eff}}{\mu_o \sigma_s}\right) - N\sigma_s\right] \quad (14)$$

μo is permeability of free space, N is the demagnetizing factor and σs is the saturation magnetization. The coercivity of our Magnetic & Dielectric Hexagonal Ceramic Oxides increases slightly from 62.85 to 75.33 Oe suggesting only slight increase in the crystalline anisotropy along easy axis of magnetization with single domain structure, rather the multi-domain structure. The critical size of single domain grain is estimated as calculated in equation – (15):

$$d_c = \frac{9\varepsilon_w}{2\pi\sigma_s^2} \quad (15)$$

The domain wall energy density is given by relation, ε_w = (2kb.Keff.Tc/a)1/2 , with Boltzmann constant, kb = 1.38x10-16 Erg/K, lattice parameter, a = 5.869 & 5.845 Å, Tc = 673 K. The calculated values of critical size and demagnetizing factor tabled in Table 7 given below:

Composition	Critical size of single domain grain (d_c)	N (Demagnetizing factor)
$Ba_{0.8}Zn_{0.2}Fe_{12}O_{19}$	129	13.930×10^7
$Ba_{0.8}Ti_{0.2}Fe_{12}O_{19}$	204	637.572×10^7

Table 7: Critical size of single domain grain (d_c) & N (Demagnetizing factor) of Magnetic & Dielectric Hexagonal Ceramic Oxides of $Ba_{0.8}Zn_{0.2}Fe_{12}O_{19}$& $Ba_{0.8}Ti_{0.2}Fe_{12}O_{19}$Nano-Ceramic Oxide

Since in M-type hexaferrite, structure has five distinct crystallographic interstitial sites, labeled as three octahedral sites (12k, 2a, $4f_2$), one tetrahedral site ($4f_1$), and one trigonal bipyramidal site (2b). The octahedral positions within the crystal structure are occupied by Fe^{3+} ions with their spins aligned in the same direction (spin-up) contributing to the magnetic properties of the material. The 12k, 2a, and 2b sites are considered "spin-up" sites, while the $4f_1$ and $4f_2$ sites are "spin-down" sites. There are two formula units per unit hexagonal unit cell of hexaferrite, wherein 12 Fe^{3+} ions are distributed in these interstitial sites. There are six ions with upward spin alignment in the 12k, one in 2a and one in 2b sites, with a total of eight Fe^{3+} ions with upward spin alignment and there are two each ion in the $4f_1$ and $4f_2$ sites, with their downward spin alignment. So, up-spins of four ions cancel-out down-spins of four ions cancel-out and the net magnetic moment accounts for the upward spins of four Fe^{3+} ions. There are only spin contributions to the magnetic moment of each Fe^{3+} ion, containing five un-paired d-electrons, accounting for magnetic moment of 5.92 Bohr magneton per ioncalculated as

$$\mu_s = \sqrt{n(n+2)}$$

Where 'n' is the number of un-pair (05) electrons in d-orbitals of Fe^{3+} ion.

Therefore, total magnetic moment per formula unit containing 12 Fe^{3+} ions with spin upward alignment of remaining four ions is 23.68 Bohr magneton and hence of unit cell of hexaferrite containing 24 Fe^{3+} ions is 47.36 Bohr magneton [24-29].

Effect of di & Tetra valence (Zn^{2+}& Ti^{4+}) substitution at Ba^{2+}in $BaFe_{12}O_{19}$of Magnetic & Dielectric Hexagonal Nano-Ceramic Oxidehave been explored for dielectric properties (ε' & ε" vs. frequency) at Room temperature. Dielectric properties (ε' & ε" vs. frequency) of Magnetic & Dielectric Hexagonal Ceramic Oxides of $Ba_{0.8}Zn_{0.2}Fe_{12}O_{19}$& $Ba_{0.8}Ti_{0.2}Fe_{12}O_{19}$have been shown in Figure 6. It has been clearly visualized from graphs that dielectric constant decreases steeply in lower frequency regime and become frequency independent after certain value of frequency leads to dielectric dispersion. The inactive response of electric dipoles towards applied alternating electric field led constant response of dielectric constant at higher frequency whereas accumulation of uncompensated surface charge at boundaries interface due to their unequal crystallite size in addition to ionic and dipolar polarization resulted in high value of dielectric constant at lower frequency. As frequency changes, change in valence state of cations and space charge polarization responsible for decrease of dielectric constant. In prepared Magnetic & Dielectric Hexagonal Ceramic Oxides of $Ba_{0.8}Zn_{0.2}Fe_{12}O_{19}$& $Ba_{0.8}Ti_{0.2}Fe_{12}O_{19}$, graphs directly reveal shift in dielectric response of prepared composites from dielectrically dispersed response to dielectrically relaxed behavior.

The slight decrease in the value of dielectric constant from ~12214 & 14961 at 1kHz to ~9656 & 14390 at 20 kHz defined as Region-I, reveals the contribution of dipolar and interfacial polarization along with electronic and ionic polarization. The further decrease of dielectric constant with its value of ~5934 & 9908 with increasing frequency upto 1.0 MHz has been labeled as region-II.This sharp decrease in value of dielectric constant in the Region-II may be resulting due to elimination of contribution of interfacial polarization, which can be explained on basis of Koop's phenomenological theory. According to this theory, in hexaferrite ceramic, dielectric properties mainly depend upon conducting grains and grain boundaries(low permittivity region)[30-34].

The high value of dielectric constant at higher frequency may be resulting due to the interchange of $Fe^{2+} \leftrightarrow Fe^{3+}$ ionsaccording to Kronig-Vick notation results in orientation polarization. At higher frequency, electron exchange between $Fe^{2+} \leftrightarrow Fe^{3+}$ does not follow externally applied alternating field and appearing of broad hump reveals that prepared Magnetic & Dielectric Hexagonal Ceramic Oxides of $Ba_{0.8}Zn_{0.2}Fe_{12}O_{19}$& $Ba_{0.8}Ti_{0.2}Fe_{12}O_{19}$tries to become dielectric relaxaor. This difference is mainly due to (a) almost frequency independent dielectric constant & (b) sharp peak at higher frequency regime corresponding to dielectric relaxation, as observed in the dielectric constant vs. Frequency profile. The high value of dielectric constant in lower frequency range resulted due to contribution of interfacial polarization due to accumulation of uncompensated charges at interfaces of conducting grains and weak conducting grain boundaries along with electronic and dipolar polarization. The large dielectric constant at high frequency range directly signature for lag in response of electron exchange between $Fe^{2+} \leftrightarrow Fe^{3+}$ with alternating applied field and orientation polarization arises due to hopping of Fe^{3+} to Fe^{2+}due to oxygen vacancies created by high temperature sintering of ceramic oxides in oxygen deficient environment as according to

$$O_0 <=> 1/2O_2 + V\ddot{}_0 + 2e'$$

This is evident from frequency dependence of dielectric constant, as shown in figure6 that prepared samples strongly impacted normal Debye behavior ofdielectrics of Magnetic & Dielectric Hexagonal Ceramic Oxides of $Ba_{0.8}Zn_{0.2}Fe_{12}O_{19}$& $Ba_{0.8}Ti_{0.2}Fe_{12}O_{19}$. The contribution of interfacial polarization along with other polarizationsincludes Ionic, Dipolar & Electronicresponsible for high value of dielectric constant in lower frequency. As frequency increases, hopping to $Fe^{3+} \leftrightarrow Fe^{2+}$ does not synchronize with applied alternating field resulted in decrease in value of dielectric constant whereas high value of dielectric constant in higher frequency resulted due to inter-conversion of $Fe^{2+} \leftrightarrow Fe^{3+}$ions in dipoles results in appearing orientation polarization due to formation of oxygen vacancies resulted due to high temperature sintering of prepared Magnetic & Dielectric Hexagonal Nano-Ceramic Oxide ceramic in oxygen deficient environment. The increased oxygen vacancies due to sintering of ceramic oxides in oxygen deficient environment. This behavior has also been direct evidence forKoop's phenomenological theory. According to this theory, dielectric properties of ceramics strongly depend upon presence of conducting grains and weekly conductinggrains boundaries. In room temperature dielectric profile, relaxation peaks predominantly appear at higher frequency with increasing ferrite content directly points towards non-Debye behavior of prepared MF ceramic composites.

$$\varepsilon'(\omega) = \varepsilon_\infty + (\varepsilon_s - \varepsilon_\infty)\frac{1 + (\omega\tau_0)^{1-\alpha}\sin\frac{1}{2}\alpha\pi}{1 + 2(\omega\tau_0)^{1-\alpha}\sin\frac{1}{2}\alpha\pi + (\omega\tau_0)^{2(1-\alpha)}}$$

$$\varepsilon''(\omega) = (\varepsilon_s - \varepsilon_\infty)\frac{(\omega\tau_0)^{1-\alpha}\cos\frac{1}{2}\alpha\pi}{1 + 2(\omega\tau_0)^{1-\alpha}\sin\frac{1}{2}\alpha\pi + (\omega\tau_0)^{2(1-\alpha)}}$$

Where ε_∞ = dielectric constant measured at high frequency, ε_s = dielectric constant measured at low frequency, $\omega = 2\pi f$ the angular frequency of applied field and τ = characteristics relaxation time of medium. The exponent parameter α usually varies between 0 and 1, and it describes the shape of spectral curves. It may be noted that for α =0, the Cole-Cole model reduces to the Debye model. [36-37].To confirm the presence of non- Debye response, dielectric data has been fitted with Havriliak–Negami relaxation model and value of □&□define whether prepared MF ceramic composites exhibits Cole-Cole Dielectric relaxation or Cole-Davidson relaxation.

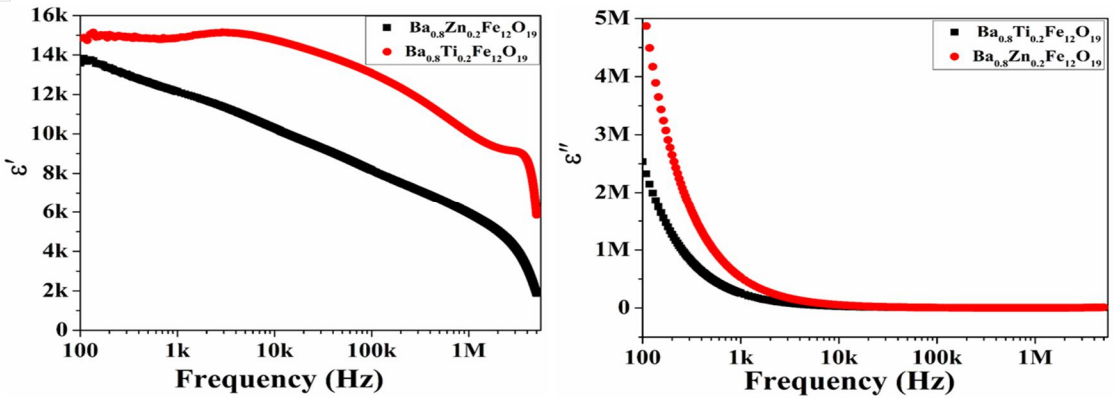

Figure 6: Room Temperature ε' & ε" vs. Frequency of Magnetic & Dielectric Hexagonal Ceramic Oxides of $Ba_{0.8}Zn_{0.2}Fe_{12}O_{19}$& $Ba_{0.8}Ti_{0.2}Fe_{12}O_{19}$Nano-Ceramic Oxide

Room Temperature Dielectric Loss (Tan □) vs. Frequency response of prepared Magnetic & Dielectric Hexagonal Ceramic Oxides of $Ba_{0.8}Zn_{0.2}Fe_{12}O_{19}$& $Ba_{0.8}Ti_{0.2}Fe_{12}O_{19}$shown in figure 7 reveals almost similar as dielectric response. In lower frequency regime, prepared MF ceramic composites exhibits high value and it decreases continuously as frequency increases and become almost constant after particular frequency. The high value of dielectric loss at lower frequency resulted due to contribution of interfacial polarization arises due to uncompensated charges accumulated at ferrite-ferroelectric interface along with other polarization (Ionic, Electronic and Dipolar) and decreases with increasing frequency evident for un-synchronization of hopping of charges (n-type and p-type) with alternating electric field. This hopping also results in orientation polarization which also contributes in dielectric loss as discussed dielectric behavior. The high value of dielectric loss also resulted due to alignment of relaxation time with time period of alternating electric field and low value at higher frequency regime appears due to hampering of domain wall motion. This hampering of domain walls may have resulted due to un-synchronization of hopping of charges (n-type and p-type) for maintaining of charge neutrality ($Fe^{3+} \leftrightarrow Fe^{2+}$) disturbed oxygen vacancies created either by substitution of valence different metal ions or by high temperature sintering of ceramic oxides in oxygen deficient environment. The dielectric loss also varies with stoichiometric proportion. The dielectric dispersed response of prepared Magnetic & Dielectric Hexagonal Ceramic Oxides of $Ba_{0.8}Zn_{0.2}Fe_{12}O_{19}$& $Ba_{0.8}Ti_{0.2}Fe_{12}O_{19}$also shown in graphs. This enhancement in dielectric loss appears due to increase in concentration in oxygen vacancies created led the polarization mechanism leads to lower loss tangent values for higher concentration of dopant at lower frequencies. The enhancement in dielectric loss also a key component which gives information about the conductive nature of prepared Magnetic & Dielectric Hexagonal Ceramic Oxides of $Ba_{0.8}Zn_{0.2}Fe_{12}O_{19}$& $Ba_{0.8}Ti_{0.2}Fe_{12}O_{19}$.

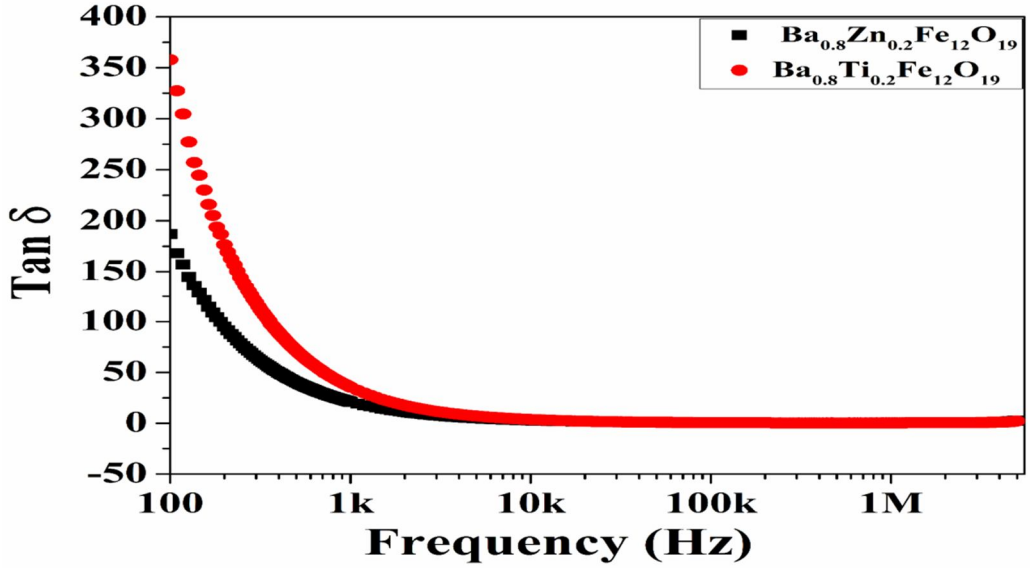

Figure 7: Room Temperature Dielectric Loss (Tan □□ vs. Frequency of Magnetic & Dielectric Hexagonal Ceramic Oxides of $Ba_{0.8}Zn_{0.2}Fe_{12}O_{19}$& $Ba_{0.8}Ti_{0.2}Fe_{12}O_{19}$Nano-Ceramic Oxide

To analyze effect of substitution of Ti^{4+} & Zn^{2+}on concentration of oxygen vacancies created, conductivity profile vs. Frequency at RT has been studied. Figure 6 shows the frequency dependence of electrical conductivity Magnetic & Dielectric Hexagonal Ceramic Oxides of $Ba_{0.8}Zn_{0.2}Fe_{12}O_{19}$& $Ba_{0.8}Ti_{0.2}Fe_{12}O_{19}$ at room temperature. The ac conductivity is calculated from the measured dielectric data using the relation:

$$\sigma ac = 2\pi f \varepsilon' \varepsilon'' Tan\delta \text{ [30]}$$

Parameters mentioned in above formula have their usual meaning. It can be observed that the ac conductivity increases with increasing frequency for all compositions. It is further clear from the figure that the conductivity shows two distinct regimes within the measured frequency limit, (i) the plateau and (ii) the dispersion region. The plateau region corresponds to low frequency region. In this region, the conductivity has been found to be independent of frequency. The dispersion region corresponds to high frequency region. In this region, conductivity increases with increase in frequency. In fact, the plateau region corresponds to dc conductivity (σ_{dc}) and dispersion region corresponds to ac conductivity (σ_{ac}). The frequency dependence of ac conductivity in ceramics is generally analyzed by Jonscher's power law [36];

$$\sigma dc + A\omega n = \sigma ac$$

Where "A" represent dispersion parameter representing strength of polarizability and "n" is dimensionless frequency exponent representing the interaction between mobile ions with the lattice around them. According to Jonscher, the origin of frequency dependence of conductivity lies in the relaxation phenomenon arising due to hoping of mobile charge carriers. Thus with increasing concentration of oxygen vacancies, the concentration of structural defects increases and hence increase in the value of conductivity.

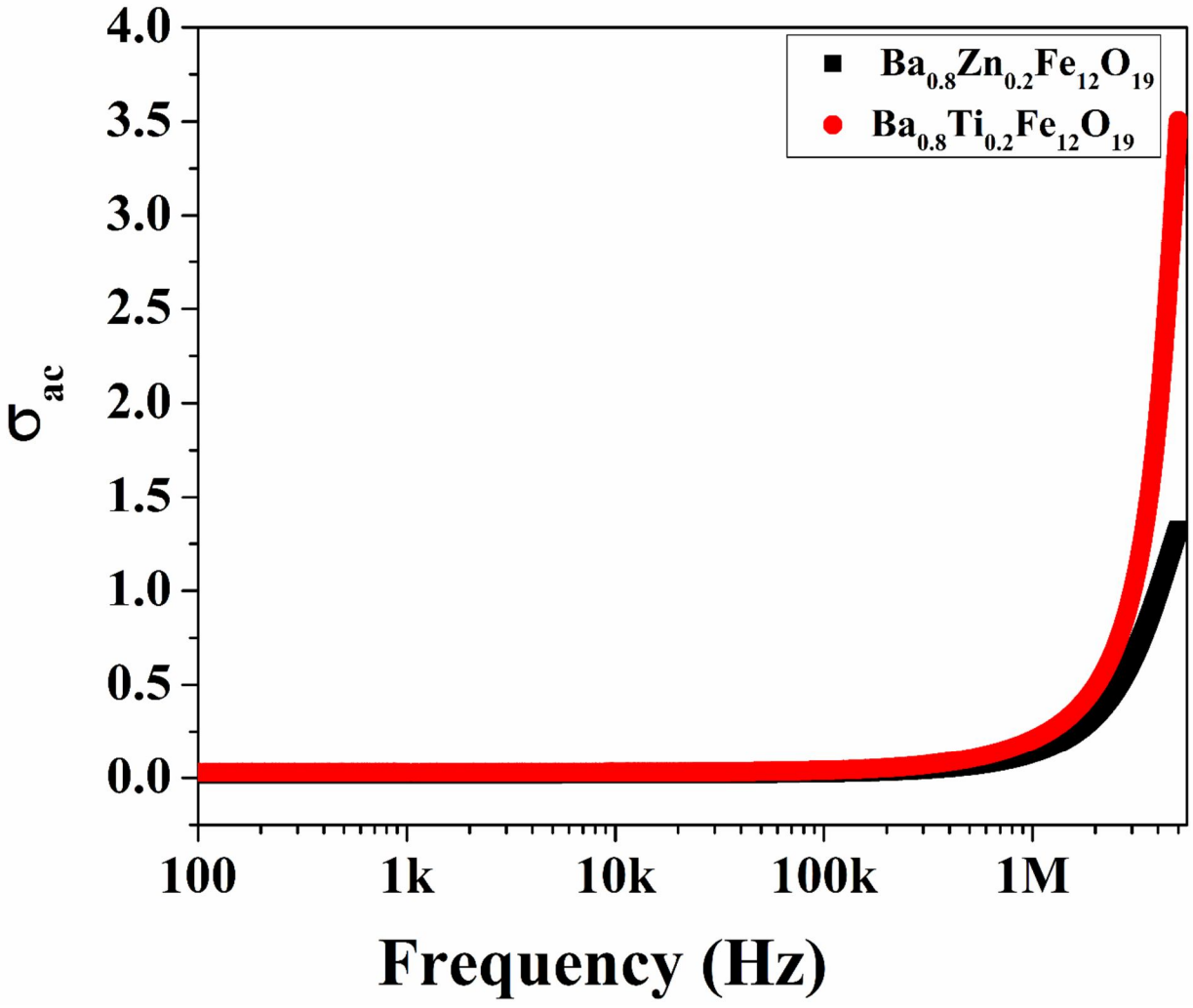

Figure 8: Room Temperature ac conductivity (□$_{ac}$□ vs. Frequency of Magnetic & Dielectric Hexagonal Ceramic Oxides of $Ba_{0.8}Zn_{0.2}Fe_{12}O_{19}$& $Ba_{0.8}Ti_{0.2}Fe_{12}O_{19}$Nano-Ceramic Oxide

IV. CONCLUSION

In the current research work, Magnetic & Dielectric Hexagonal Ceramic Oxides of $Ba_{0.8}Zn_{0.2}Fe_{12}O_{19}$& $Ba_{0.8}Ti_{0.2}Fe_{12}O_{19}$have been synthesized using Auto-Combustion approach and characterize forstructural, microstructural, optical, luminescence, magnetic & dielectric properties. Diffraction peak positioned at 2θ ~ 34.11 signature for crystallization of prepared Nano ceramic oxides in hexagonal crystal phase with space group $P6_3/mmc$ No. 194withincreasing crystallite size from ~91 to 102 nm whereas porosity of ~ 3%.

The increase of magnetic characteristic (M_r) reveals direct influence of Zn^{2+}& Ti^{4+}substitution as compared to pure $BaFe_{12}O_{19}$ hexaferrite due to increase of oxygen vacancies due to aliovalent substitution of Ti^{4+} as compared to Zn^{2+} at Ba^{2+} in $BaFe_{12}O_{19}$ hexaferrites. Square-ness ratio (M_r/M_s = >0.5 &< 1) shows multi-domain structure with presence of ferromagnetic ordering whereas change in value of magnetic moment (η_B) reveals magnetic behavior resulted due to up & down spin of Fe^{3+} coupled at octahedral and tetrahedral sites. Broad peak in wavelength ranging from 375 to 475 nm strongly reveals presence of ferromagnetic oxide ($BaFe_{12}O_{19}$ in our prepared Magnetic & Dielectric Ceramics) whereas increased conductivity shows that prepared Nano-Ceramic Oxide useful for Capacitive Applications

REFERENCES

[1] Guolong Tann, Xiuna Chen, Structure and multiferroic properties of barium hexaferrite ceramics, Journal of Magnetism and Magnetic Materials 327 (2013) 87–90
[2] Meera Rawat and K L Yadav, Electrical, magnetic and magnetodielectric properties in ferrite-ferroelectric particulate composites, IOP Publishing, Smart Materials and Structures, Smart Mater. Struct. 24 (2015) 045041 (11pp) doi:10.1088/0964-1726/24/4/045041
[3] Ayesha Khalid, Ghulam M. Mustafa, Shahzad Naseem, Shahid Atiq, Sm-mediated dielectric characteristics and tunable magneto-electric coefficient of $0.5Bi_{1-x}Sm_xFe_{0.95}Mn_{0.05}O_3$-$0.5PbTiO_3$ composites, Ceramics International 45 (2019) 7690-7695
[4] Himani Joshi, A. Ruban Kumar, Investigations and Correlations of Structural, Magnetic, and Dielectric Properties of M-Type Barium Hexaferrite ($BaFe_{12}O_{19}$) for Hard Magnet Applications, Journal of Superconductivity and Novel Magnetism (2022) 35:2435–2451 https://doi.org/10.1007/s10948-022-06203-x
[5] Impact of Nd^{3+} Substitutions on the Structure and Magnetic Properties of Nanostructured SrFe12O19 Hexaferrite Ashraf M. Semaida, Moustafa A. Darwish, Sergei V. Trukhanov, MohamedM.Salem3,DiZhou4 , Alex V. Trukhanov, Vladimir P. Menushenkov, Tatiana I. Zubar , and Alexander G.Savchenko, Nanomaterials (Basel)2022 Oct 2;12(19):3452, doi: 10.3390/nano12193452.
[6] Debesh D. Mishra, Daniel M. Tewelde, Min Wang, Guolong Tan, Multiferroic properties of $PbFe_{12}O_{19}$–$PbTiO_3$ composite ceramics, Journal of Materials Science: Materials in Electronics https://doi.org/10.1007/s10854-019-01426-6a
[7] Melvin M. Vopson , Fundamentals of Multiferroic Materials and Their Possible Applications, Critical Reviews in Solid State and Materials Sciences, 40:223–250, 2015
[8] Dhiren K. Pradhan, Shalini Kumari and Philip D. Rack, Magnetoelectric Composites: Applications, Coupling Mechanisms, and Future Directions, Nanomaterials 2020, 10(10), 2072; https://doi.org/10.3390/nano10102072
[9] Khomskii DI (2006) Multiferroics: Different ways to combine magnetism and ferroelectricity. J Magn Magn Mater 306:1–8. https://doi.org/10.1016/j.jmmm.2006.01.238
[10] Mehak Arora, Shubpreet Kaur, Sunil Kumar, Khalid Bujasam Batoo, Sajjid Hussain, Anupinder Singh, Establishment of magneto-electric response in $GdFeO_3$ doped $PbTiO_3$ solid Solutions, Ceramic International, Vol. 50 Issue 7 Part A, 10117-10130 (2024)
[11] Mehak Arora, Shubhpreet Kaur, Sunil Kumar, Parambir Singh Malhi, Mandeep Singh andAnupinder Singh, Evaluation of Dielectric, Energy storage and multiferroic properties of $PrFeO_3$-$PbTiO_3$ solid solutions, Journal of Advanced Dielectrics, Vol. 12, No. 5 (2022) 2250012 (13 pages)
[12] Sunil Kumar, Jaswinder Pal, Shubhpreet Kaur, Parambir, Singh Malhi, P.D. babu, Mandeep Singh and Anupinder Singh Compositional dependent Multiferroic and Magnetoelectric Properties of $NdFeO_3$-$PbTiO_3$ Solid Solutions, Journal of Asian Ceramic Societies, Vol. 9 (2021) 185-197
[13] Sunil Kumar, Jaswinder Pal, Shubhpreet Kaur, Sajjan Dahiya, Tulika Maitra, AvijeetRay, P.D. babu, Mandeep Singh and Anupinder Singh Correlation between Multiferroic Properties and Processing Parameters in $NdFeO_3$-$PbTiO_3$ Solid Solutions, Journal of Alloys and Compounds, Vol. 764 824-833 (2018), 10.1016/j.jallcom.2018.06.058
[14] Spaldin NA, Fiebig M (2005) The Renaissance of Magnetoelectric Multiferroics. Mater Sci 309:391–392
[15] Eerenstein W, Mathur ND, Scott JF (2006) Multiferroic and magnetoelectric materials. Nature 442:759–765. https://doi.org/10.1038/nature05023
[16] Mirza Bichurin, Vladimir Petrov, Shashank Priya, and Amar Bhalla, Multiferroic Magnetoelectric Composites and Their Applications, Hindawi Publishing Corporation Advances in Condensed Matter Physics Volume 2012, Article ID 129794, 3 pages doi:10.1155/2012/129794
[17] Himani Joshi, A. Ruban Kumar, Investigations and Correlations of Structural, Magnetic, and Dielectric Properties of M-Type Barium Hexaferrite ($BaFe_{12}O_{19}$) for Hard Magnet Applications, Journal of Superconductivity and Novel Magnetism (2022) 35:2435–2451 https://doi.org/10.1007/s10948-022-06203-x
[18] Al Dairy AR, Al-Hmoud LA, Khatatbeh HA (2019) Magnetic and structural properties of Barium Hexaferrite nanoparticles doped with Titanium. Symmetry (Basel) 11:1–11. https://doi.org/10.3390/sym11060732
[19] Guolong Tann, Xiuna Chen, Structure and multiferroic properties of barium hexaferrite ceramics, Journal of Magnetism and Magnetic Materials 327 (2013) 87–90
[20] Ajay Singh, Balwinder Kaur, Manju Arora, Vishal Singh, Effect of $PbTiO_3$ concentration on structural, paramagnetic resonance and magnetoelectric properties of $PbTiO_3$:$SrFe_{12}O_{19}$ multiferroic nanocomposites , Materials Chemistry and Physics 258(2021)123849
[21] Ajay Singh, Vishal Singh, K.K. Bamzai, Structural and magnetic studies on $_{(x)}PbTiO_3$ - $_{(1\ x)}SrFe_{12}O_{19}$ composite multiferroics, Materials Chemistry and Physics 155 (2015) 92-98

[22] Ruoshui Liu, Lichen Wang, Xiang Yu, Zhiyi Xu, Huayang Gong, Tongyun Zhao, Fengxia Hu, Baogen Shen, Magnetocrystalline anisotropy study of Co-substituted M-type strontium hexaferrite single crystals, CeramicsInternational49(2023)1888–1895
[23] B. C. Brightlin and S. Balamurugan, Magnetic, Micro-structural, and Optical Properties of Hexaferrite, BaFe12O19 Materials Synthesized by Salt Flux-Assisted Method B. C. Brightlin1 · S. BalamuruganMagnetic, Micro-structural, and Optical Properties of Hexaferrite, BaFe12O19 Materials Synthesized by Salt Flux-Assisted Method, J Supercond Nov Magn DOI 10.1007/s10948-016-3703-z
[24] Ihsan Ali , M.U. Islam, M.S. Awan, Mukhtar Ahmad , Effects of Ga–Cr substitution on structural and magnetic properties of hexaferrite ($BaFe_{12}O_{19}$) synthesized by sol–gel auto-combustion route, Journal of Alloys and Compounds 547 (2013) 118–125
[25] Ihsan Ali, M.U. Islam, M.S. Awan, Mukhtar Ahmad , Muhammad Naeem Ashiq , Shahzad Naseem, Effect of Tb3+ substitution on the structural and magnetic properties of M-type hexaferrites synthesized by sol–gel auto-combustion technique, Journal of Alloys and Compounds 550 (2013) 564–572
[26] A. Baykala, I.A. Auwalb, S. Günerc, H. Sözeri, Magnetic and optical properties of Zn^{2+} ion substituted barium hexaferrites, Journal of Magnetism and Magnetic Materials 430 (2017) 29–35
[27] S. Asiri, S. Güner, A.D. Korkmaz, Md. Amird, K.M. Batooe, M.A. Almessiere, H. Gungunes, H. Sözeri, A. Baykal, Magneto-optical properties of $BaCr_yFe_{12-y}O_{19}$ ($0.0 < y < 1.0$) hexaferrites , JournalofMagnetismandMagneticMaterials451(2018)463–472
[28] Ajay Singh, Shivani Suri, Balwinder Kaur, Parveen Kumar , Anil K. Thakur, Vishal Singh, Effect of temperature and frequency on electrical properties of composite multiferroic of lead titanate and strontium hexaferrite ($PbTiO_3 – SrFe_{12}O_{19}$), Journal of Alloys and Compounds 812 (2020) 152254
[29] GURPREET SINGH, HARJEET KAUR, SAJAN MASIH, ARSHDEEP KAUR, SHIFFALI MIDDHA, SUNIL KUMAR, JASVIR SINGH, JAHANGEER AHMED, JAVIER LOPEZ GARCIA, SATVIR SINGH, NITIN TANDON, INDU SHARMA and ANUPINDER SINGH, Exploration on magnetic, dielectric and magnetodielectric properties of PNZT-strontium hexaferrite composites, Bull. Mater. Sci. (2025) 48:97, https://doi.org/10.1007/s12034-025-03452-z]
[30] Kumar M, Yadav KL. J. Phys.: Condens. Matter. 2002;19:242202.
[31] Cole KS, Robert H. Dispersion and Absorption in Dielectrics:- Alternating Current Characteristics. Journal of Chemical Physics. 1941;9:341–351.
[32] Havriliak S, Negami S. A complex plane representation of dielectric and mechanical relaxation processes in some polymers. Polymer. 1967;8:161-210. DOI: 10.1016/0032-3861 (1967) 90021-3.
[33] JonscherAK. The Universal dielectric response. Nature. 1977;267:673-679.
[34] Prakash V, Choudhary SN, Sinha TP. Dielectric relaxation in complex perovskite oxide BaCo1/2W1/2O3. Physica B. 2008;403:103–108.
[35] V.R. Palkar, D.C. Kundaliya, S.K. Malik and S. Bhattacharya, Magnetoelectricity at room temperature in $Bi_{0.9-x}Tb_xLa_{0.1}FeO_3$ system, Phys. Rev. B. 69 (2004)212102-3.
[36] M. Kumar and K.L. Yadav, Study of dielectric, magnetic, ferroelectric and Magnetoelectric properties in the $PbMn_xTi_{1-x}O_3$ system at room temperature, J. Phys: Condens. Mater 19 (2007) 242202 (1-7 pages)

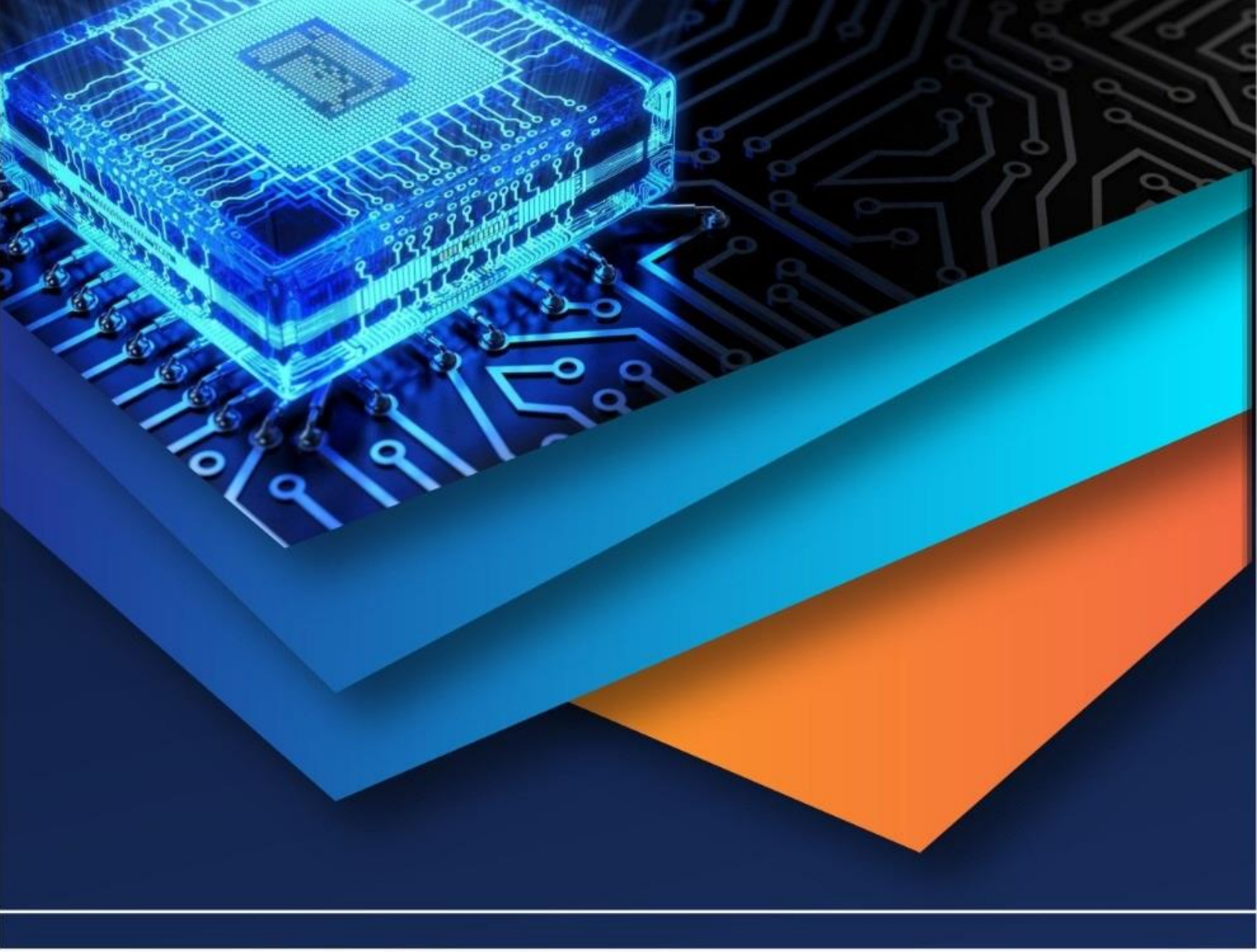

10.22214/IJRASET

45.98

IMPACT FACTOR: 7.129

IMPACT FACTOR: 7.429

INTERNATIONAL JOURNAL FOR RESEARCH

IN APPLIED SCIENCE & ENGINEERING TECHNOLOGY